23rd IMEKO TC4 International Symposium
Electrical & Electronic Measurements Promote Industry 4.0
September 17-20, 2019，Xi'an, China

Displacement Measurements in UME Oscillating-Magnet Kibble Balance

H Ahmedov, M Çelik, R Orhan, B Korutlu, R Hamid, E Şahin

TÜBİTAK National Metrology Institute (UME), Kocaeli, TURKEY, haji.ahmadov@tubitak.gov.tr

Abstract –
The redefinition of kilogram in terms of Planck constant rather than a physical artifact of International Prototype of Kilogram will be put into force in May 20th, 2019. National Metrology Institute of Turkey contributes to the ongoing worldwide scientific work on the realization of kilogram with an Oscillating-Magnet Kibble Balance experiment. The novel dynamical measurement procedure developed for Kibble Balance Experiment in Turkey poses the advantage of being less sensitive to the environmental disturbances. Precise displacement measurements between the coil suspended from a balance and the surrounding magnetic circuit are vital to reach the required uncertainties in the realization experiments via Kibble balance. The Michelson Interferometer and the Fabry-Perot Interferometer are commonly used in precise displacement measurements in worldwide Kibble balances. A commercial, miniature, plane mirror Michelson Interferometer with compact sensor head is used in the Kibble Balance Experiment of Turkey. In this paper, we determine the contribution of ultra-small oscillations to Planck constant by taking simultaneous displacement measurements on two back-to-back mirrors attached to the piezoelectric transducer undergoing an oscillatory motion with Michelson Interferometer and Fabry-Perot Interferometer. Although, in the specification of these instruments it has been stated that extreme precautions are required in the environmental conditions to be able to measure displacements with ultra-small amplitudes, following the novel measurement procedure makes such measurements possible in a regular laboratory environment which allows us to investigate the resolution performance of these instruments in laboratory conditions. Consistent results with resolution uncertainties of 1.4×10^{-9} and 2.2×10^{-9} are obtained for Michelson Interferometer and the Fabry-Perot Interferometer, respectively. As the expected relative uncertainty in the redefinition experiments of the kilogram is above the resolution uncertainties of both interferometers, we may conclude that a commercial, miniature, plane mirror Michelson Interferometer with compact sensor head will serve for our purposes in the route for the redefinition of kilogram.

Keywords – Kibble Balance, Planck Constant, Interferometer, SI Unit, Resolution Uncertainty

I. INTRODUCTION

In November 16th, 2018 an epoch making decision on the redefinition of kilogram has been voted by the Member States of International Bureau of Weights and Measures (BIPM) at the 26th meeting of The General Conference on Weights and Measures (CGPM) held in Versailles, France. Based on the affirmative voting in the 26th CGPM meeting, effective from May 20th, 2019 Planck constant with fixed value of $h = 6.626\ 070\ 15 \times 10^{-34}$ J s will be used in the new definition of kilogram ensuring uniform, world-wide accessible, long-term stable unit for mass measurements rather than a physical artifact with limited access and quantitative limitations - namely the International Prototype of Kilogram (IPK). The new definition of kilogram can be realized via the Kibble Balance experiment [1] by comparing electrical power to the mechanical one with the help of two macroscopic electrical quantum phenomena: the Quantum Hall Effect [2] and the Josephson Effect [3]. Different construction and operating modes in Kibble balance experiments (see [4] and references therein) are favorable for better understanding of the possible systematic errors. TÜBİTAK National Metrology Institute (UME) of Turkey contributes to the ongoing worldwide scientific work on the redefinition of kilogram with an Oscillating-Magnet Kibble Balance Experiment where its novel dynamical measurement procedure, makes the system less sensitive to the environmental disturbances [5-7].

All existing Kibble Balances consist of a coil suspended from a balance embedded in a strong magnetic field created by permanent magnetic circuit. The relative motion between the coil and the magnetic circuit induces a Faraday's voltage across the ends of the coil. The precise measurements of the displacement and the voltage are vital to be able to achieve the required total relative uncertainty of 2×10^{-8} in the kilogram realization experiments with Kibble Balance systems. The content of this paper focuses mainly on the displacement

measurements. In the Kibble Balance experiments, Laser Interferometers, e.g. the Michelson Interferometer (MI) [8-14] and the Fabry-Perot Interferometer (FPI) [15] are used to measure the displacement between the magnetic circuit and the coil (see Table 2 in [4] and references therein). In the MI, the laser beam is split into two perpendicular arms, the reference arm and the measurement arm, and recombines at the beam splitter after being reflected by the reference and measurement reflectors, respectively. The phase differences between the two beams are influenced by tiny variations in environmental changes, as they follow different optical paths. The FPI, on the other hand, includes only one arm with two parallel mirrors aligned to form an optical resonator. As it features a common optical path, the FPI is less sensitive to environmental disturbances compared to MI [16]. In traditional Kibble Balances, extreme precautions are taken for eliminating the environmental disturbances on the displacement measurements which complexifies the experimental set-up.

In this paper, we apply the dynamical measurement procedure developed for UME Oscillating-Magnet Kibble Balance Experiment on interferometric displacement measurements performed simultaneously by MI and FPI. We are mainly concerned with the measurement capabilities of MI for ultra small displacements where environmental disturbances are prevailing. FPI is used in order to justify the ultra small displacement measurements by MI. The results indicate that the parasitic effect by the environmental disturbances on the measurement precision of MI is immune provided that the aforementioned measurement procedure is followed. This allows us to use a commercial miniature plane mirror MI with compact sensor head for the precision displacement measurements in UME Oscillating-Magnet Kibble Balance.

II. MEASUREMENT PROCEDURE

UME oscillating magnet Kibble balance consists of a stationary coil suspended from the handler of the mass comparator and a mass standard of 1 kg on the handler. The coil is placed in the air gap of an oscillating magnetic circuit along the direction of the gravitational acceleration. Ampere's Force Law and Faraday's Law of Induction play central roles in this configuration such that the gravitational force on the mass standard is counter balanced by the Lorentz force F, created on the coil carrying a DC current J, through radially outward magnetic flux density and the oscillating magnetic circuit with a velocity $u(t)$ induces an AC Faraday's voltage $V(t)$ across the ends of the coil. Combining these two laws and assuming the velocity $u(t)$ to be directed along the direction of gravitational acceleration (no horizontal or angular motions) one may write

$$\frac{h}{h_c} V(t) = G\ u(t), \tag{1}$$

where h is the actual Planck constant, h_c is the consensus value of the Planck constant as was announced in the 26th CGPM meeting. The ratio h/h_c on the left hand side of (1) appears due to the fact that the voltage and resistance are measured based on the Josephson and Klitzing constants determined by using the consensus value of the Planck constant. $G = F/J$ is the geometrical factor which depends on the structure of the magnetic flux density and the geometry of the coil.

In the context of this paper, we may neglect the inhomogenities of geometrical factor in the vertical direction. Under this assumption, the measurement procedure followed in UME Kibble Balance yields

$$\frac{h}{h_c} = G\ \{z|W\}, \tag{2}$$

where $z = \int u\,dt$ is the displacement of the magnet, $W = \int V\,dt$ is magnetic flux passing through the coil and

$$\{z|W\} = \frac{1}{2N} \sum_{k=1}^{2N} \frac{z_{k+1} - z_k}{W_{k+1} - W_k}, \tag{3}$$

represents the averaging of displacement over the magnetic flux (see [6] for details). The integration time of the Kibble balance experiment is chosen to be a multiple of the fundamental period of oscillation. We divide the integration time into $2N$ half-cycles, denoted by k. One half-cycle is the region between the consecutive displacement extrema. For the k[th] half-cycle, z_k is the preceding extrema while z_{k+1} is the succeeding one as shown in Fig.1. The corresponding W_k and W_{k+1} values are taken at the displacement extremum points.

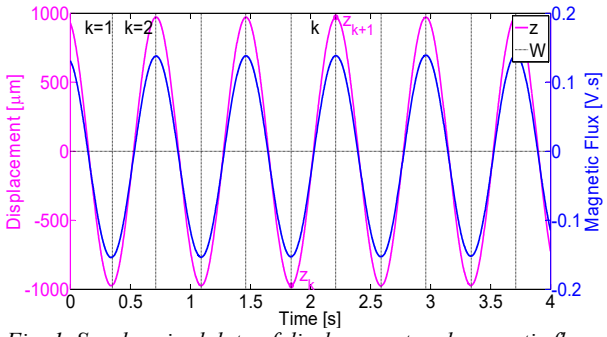

Fig. 1. Synchronized data of displacement and magnetic flux. The small portion of data is presented for better illustration of half-cycles.

Using (1) and (2) we obtain

$$\frac{h^{(m)}}{h} = \left\{z^{(m)}\middle|z\right\}, \tag{4}$$

where the parameters with the superscript (m) are the

measured values and the ones without superscript are the actual values of the corresponding parameters. The ratio of the measured Planck constant to the actual one is equal to the averaging of the measured displacement over the actual displacement. An ideal displacement measurement device would give this ratio to be equal to one. Any deviations from this value represent the inaccuracies of the measurement device. As we are interested in determining displacement measurement uncertainties, in deriving (4) we assumed that the uncertainties on all other contributing parameters (i.e., electrical current, voltage, mass and gravity) are carried with accuracies sufficient for the realization of kilogram.

The resolution of a measurement instrument is an essential property as it describes the smallest measurable quantity. In this paper, we investigate the reading performance of the commercial Michelson Interferometer used in UME Kibble Balance experiment. To serve for our purposes, we use a sinusoidal reference signal with ultra-small amplitude. As a reference signal z, we use the oscillation produced by the piezoelectric transducer (PZT). High stability of PZT allows us to describe the reference signal by only three parameters: fundamental oscillation frequency f, oscillation amplitude A and phase φ such that

$$z(t) = A\cos(2\pi f t + \varphi). \qquad (5)$$

The fundamental oscillation frequency f and the phase φ are obtained by signal processing followed in the next section. The oscillation amplitude A is chosen to be close to the resolution of the MI. Since we neglect uncertainty over the full scale, we do not need to measure the amplitude A of the ultra-small oscillations exactly. We may rescale it to a desired value. In our analysis, we rescale the oscillation amplitude of PZT to be equal to the one of the magnetic circuit in UME Kibble Balance experiment. In this case (4) defines the contribution of ultra-small amplitude oscillations to the Planck constant and its uncertainty defines the resolution uncertainty. In the rest of the paper, we call contribution of ultra-small amplitude oscillations to the Planck constant in short as *Ultra-Small Oscillation Contributions*.

III. RESULTS AND DISCUSSIONS

The experimental set-up consists of SIOS AE SP 2000E miniature plane mirror Michelson Interferometer and UME-made Fabry-Perot Interferometer [17-18] as shown in Fig. 2. Two back-to-back mirrors attached to the piezoelectric transducer undergo an oscillatory motion. The frequency and amplitude of this motion is supplied by the AC voltage applied on the PZT by the function generator. The reading performance of MI is tested by using reference signal with amplitude of about 10 pm. This value is given in the specifications of the device as resolution. In order to reach such ultra-small amplitudes, in-line attenuators are used at the output of the function generator.

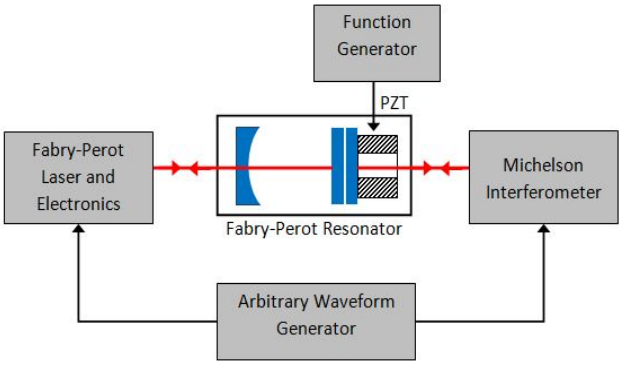

Fig. 2. The schematic diagram of experimental set-up.

The oscillations of about 1 Hz are measured by the FPI and the MI simultaneously for the time interval of 500 s. Keysight 33512B Two-Channel Arbitrary Waveform Generator is used for synchronization of FPI and MI data samplings of 50 Hz. The displacement data for MI (z_n^M) and FPI (z_n^{FP}) are shown in Fig. 3. The signal discretization index n runs from 1 to $N = 25000$.

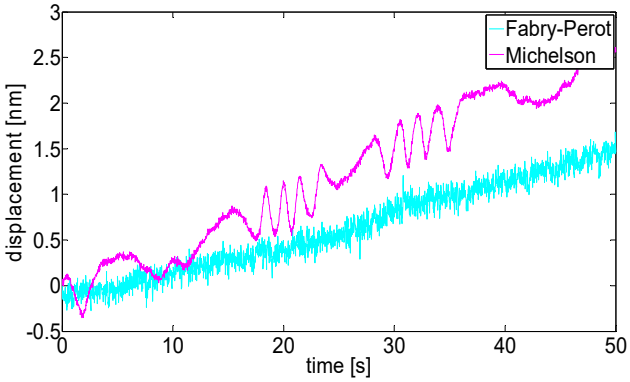

Fig. 3. Displacement data measured by FPI (cyan) and MI (magenta). For illustration purposes, only a portion of data is shown.

In order to estimate the fundamental oscillation frequency f and the phase φ of the reference signal encoded in these curves, it is useful to decompose the data into two parts as digitally band-pass filtered data and its residual. Digitally band-pass filtered data $\tilde{z}_n^{M(FP)}$ is of the form

$$\tilde{z}_n^{M(FP)} = \frac{1}{2l+1}\sum_{s=-l}^{l} z_{n+s}^{M(FP)}, \qquad (6)$$

where $2l+1$ is obtained by taking the ratio of the oscillation frequency to the sampling frequency and $n = l+1, \cdots, N-l$. The digitally band-pass filtered data given in Fig. 4 describes low frequency processes which are caused mainly by environmental disturbances.

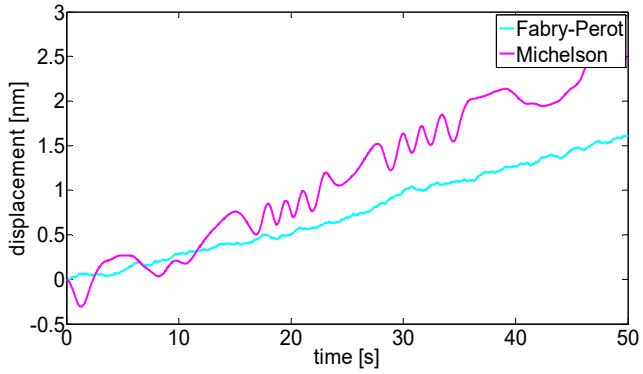

Fig. 4. Low-pass filtered data of FPI (cyan) and MI (magenta). For illustration purposes, only a portion of data is shown.

Four parameter sine-fit algorithm (FPSF) [19] is performed for determining the amplitude, frequency and phase of the residual data measured by MI and FPI. The results are summarized in Table 1.

Table 1. The frequency, amplitude and phase obtained by the FPSF algorithm applied on FPI and MI residual data.

Parameters	FPI	MI	Difference
Frequency (Hz)	1.00036	0.99987	0.00049
Amplitude (pm)	8.5	8.1	0.4
Phase (rad)	1.17	1.10	0.07

The residual FPI and MI data and the reconstructed signal by FPSF algorithm are given in Fig. 5 and Fig. 6, respectively.

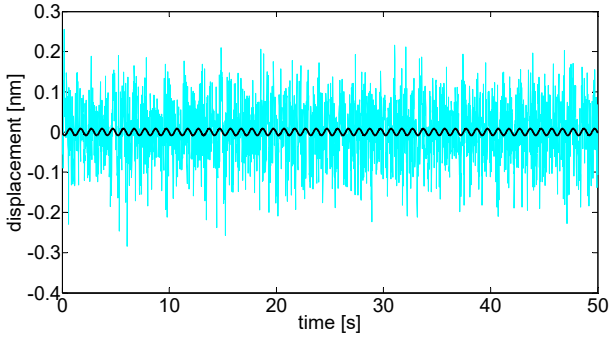

Fig. 5. The residual data (cyan) measured by FPI and the estimation of reconstructed signal by FPSF algorithm performed on the residual data of FPI (black). For illustration purposes, only a portion of data is given.

The findings of the analysis indicate that, the estimated parameters by FPSF algorithm on MI and FPI residual data are quite close to each other (see Table 1). This is a strong indication of the consistency between the interferometric measurements by MI and FPI. The differences occur due to the low signal to noise ratio of about -20 dB in the residual data. It is reasonable to assume that the actual phase and frequency values are in close proximity to the obtained ones for the reference signal.

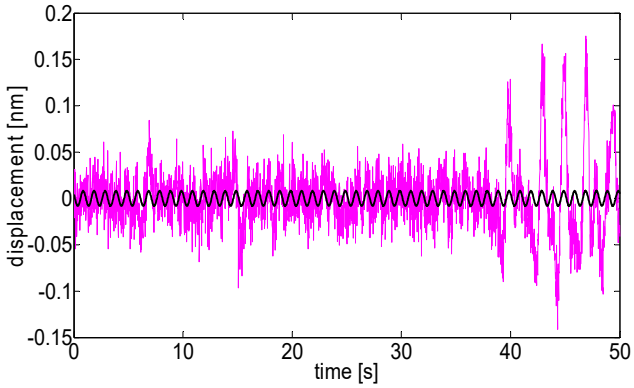

Fig. 6. The residual data (magenta) measured by MI and the estimation of reconstructed signal by FPSF algorithm performed on the residual data of MI (black). For illustration purposes, only a portion of data is given.

To establish the resolution performance of the interferometers for ultra small oscillations, we divide the raw data $z^{MI(FPI)}$ of 500 s into 5 independent measurement sets of 100 s and represent each set of displacement data by $z_s^{MI(FPI)}$ where $s = 1, \cdots, 5$. The ratio $h_s^{MI(FPI)}/h$ is determined for each set using (4). The mean value of these sets defines the contribution of ultra-small amplitude oscillations contributing to the Planck constant and the standard deviation defines the resolution uncertainty.

As it is summarized in Table 1, the interferometric measurements of ultra-small oscillations by MI and FPI are close to each other. Therefore, it is reasonable to expect the ratio h_s^{MI}/h to be close to the ratio h_s^{FPI}/h. In consequence, one may perform the following optimization procedure for estimating the parameters of reference signal. As a first step, an optimization function

$$F(f,\varphi) = \sum_{s=1}^{5} \left(\frac{h_s^{FPI}}{h} - \frac{h_s^{MI}}{h} \right)^2, \qquad (7)$$

is introduced. Then, using the optimization function, $F(f,\varphi)$, a 100 by 100 matrix is constructed in light of the reconstructed signals, by increments of 0.00001 Hz for the frequency range from 0.99950 Hz to 1.00050 Hz and by increments of 0.01 rad for the phase range from 0.65 rad to 1.65 rad. The estimated values for the reference signal are obtained to be $f = 1.00023$ Hz and $\varphi = 0.95$ rad as they are the numerical values making the difference in (7) minimum. Fig 8 summarizes the ultra-small oscillation contributions obtained for each set s. The resolution uncertainties for the FPI and MI and the corresponding mean values determining the ultra-small oscillation contributions are summarized in Table 2. It is important to emphasize that even though the followed optimization procedure makes the results by MI and FPI to fit better, the mean value and the uncertainties obtained without

optimization procedure are still below 10^{-9}.

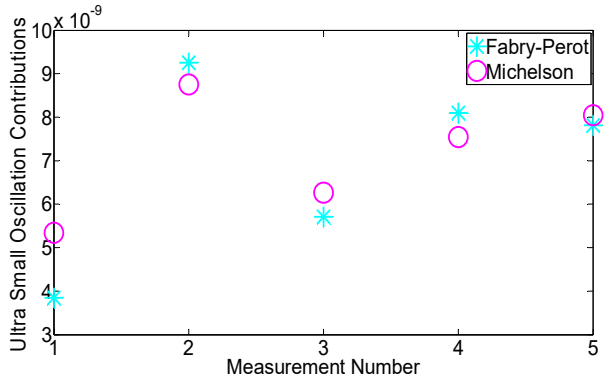

Fig. 8. The contribution to $h_s^{MI(FPI)}/h$ obtained by simultaneous measurements with MI (circles in magenta) and FPI (stars in cyan).

Table 2. The mean values for the ultra-small oscillation contributions and resolution uncertainties for FPI and MI.

Parameters	FPI	MI
Mean	6.9×10^{-9}	7.2×10^{-9}
Standard Deviation	2.2×10^{-9}	1.4×10^{-9}

IV. CONCLUSIONS

In this paper, we apply the dynamical measurement procedure developed for UME Oscillating-Magnet Kibble Balance to interferometric displacement measurements performed simultaneously by MI and FPI to test the resolution performance of MI. The analysis of data yields the mean values for the ultra-small oscillation contributions to be 6.9×10^{-9} and 7.2×10^{-9} and the resolution uncertainties to be 2.2×10^{-9} and 1.4×10^{-9}, for FPI and MI, respectively. As the relative uncertainty for the redefinition experiments of the kilogram is expected to be 2×10^{-8}, the ultra-small oscillation contribution and the resolution uncertainty obtained for the commercial miniature plane mirror MI will serve for our purposes without taking extreme precautions for eliminating the environmental disturbances on the displacement measurements. The parasitic effects are eliminated simply by performing the dynamical measurement procedure developed for UME Kibble Balance Experiment.

V. ACKNOWLEDGMENT

This research is funded by TÜBİTAK National Metrology Institute of Turkey.

REFERENCES

[1] Kibble, B P and Robinson, I A, *Feasibility study for a moving coil apparatus to relate the electrical and mechanical SI units*, Technical Report DES, vol. 40, NPL, 1977.

[2] von Klitzing, K, Dorda, G and Pepper, M, *New method for high accuracy determination of the fine-structure constant based on quantised Hall resistance*, Phys. Rev. Lett., vol. 45, 1980, pp. 494–7.

[3] Josephson, B D, *Possible new effects in superconductive tunneling*, Phys. Lett., vol. 1, 1962, pp. 251–3.

[4] Robinson, I A and Schlamminger S, *The watt or Kibble balance: a technique for implementing the new SI definition of the unit of mass* Metrologia, vol. 53, 2016, pp. A46–74.

[5] Ahmedov, H, *An Oscillating magnet watt balance*, CPEM 2016 Conf. Digest, 2016.

[6] Ahmedov, H, Babayiğit Aşkın, N, Korutlu, B and Orhan, R, *Preliminary Planck constant measurements via UME oscillating - magnet Kibble balance*, Metrologia, vol. 55, 2018, pp. 326-333.

[7] Ahmedov, H, Korutlu, B and Orhan, R, *Optimization Procedure for Faraday's Voltage in UME Kibble Balance*, IEEE Transactions on Instrumentation and Measurement, vol. 68, no. 6, 2019, pp. 2172-2175.

[8] Bielsa, F, Robertsson, L, Lavergne, T, Kiss, A, Fang, H and Stock, M, *The new interferometer of the BIPM watt balance*, Conference on Precision Electromagnetic Measurements (CPEM 2016), Ottawa, ON, 2016, pp. 1-2.

[9] Kim, D, Woo, B, Lee, K, Choi, K, Kim, J, Wan, K, Kim, J, *Design of the KRISS watt balance*, Metrologia, vol. 51, 2014.

[10] Thomas, M, Ziane, D, Pinot, P, Karcher, R, Imanaliev, A, Pereira Dos Santos, F, Merlet, S, Piquemal, F and Espel, P, *A determination of the Planck constant using the LNE Kibble balance in air,* Metrologia, vol. 54, 2017, pp. 468-480.

[11] Sutton. C M, *An oscillatory dynamic mode for a watt balance*, Metrologia, vol. 46, 2009, pp. 467-472.

[12] Robinson, I A, *Towards the redefinition of the kilogram: a measurement of the Planck constant using the NPL Mark II watt balance*, Metrologia, vol. 49, 2011, pp. 113-156

[13] Wood,B M, Sanchez, C A Green, R G and Liard, J O, *A summary of the Planck constant determinations using the NRC Kibble balance*, Metrologia, vol. 54, 2017, pp. 399-409.

[14] Haddad, D, Seifert, F, Chao, L S, Possolo, A, Newell, D B, Pratt, J R, Williams, C J and Schlamminger, S, *Measurement of the Planck constant at the National Institute of Standards and Technology from 2015 to 2017,* , Metrologia, vol. 54, 2017, pp. 633-641.

[15] Eichenberger, A, Baumann, H, Jeanneret, B, Jeckelmann, B, Richard, P and Beer, W, *Determination of the Planck constant with the METAS watt balance*, Metrologia, vol. 48, 2011, pp. 133–41.

[16] Yung-Cheng, W, Lih-Horng, S and Chung-Ping, C, *The Comparison of Environmental Effects on Michelson and Fabry-Perot Interferometers Utilized for the Displacement Measurement*, Sensors, vol. 10, 2010, pp. 2577-2586.

[17] Celik, M, Hamid, R, Kuetgens, U, & Yacoot, A, *Picometre displacement measurements using a differential Fabry–Perot optical interferometer and an x-ray interferometer*, Measurement Science and Technology, vol. 23, no.8, 2012, pp.085901.

[18] Pisani, M, et. al., *Comparison of the performance of the next generation of optical interferometers*, Metrologia, vol. *49, no.*4,2012, pp. 455.

[19] Händel, P, *Properties of the IEEE-STD-1057 Four-Parameter Sine Wave Fit Algorithm*, IEEE Transactions on Instrumentation and Measurement, vol. 49, no. 6, 2000, pp. 1189-93.